



**HAL**  
open science

## Interaction of plasma generated carbon monoxide (CO) with mouse blood hemoglobin

Claire Douat, Pablo Escot Bocanegra, Sébastien Dozias, Robert Eric, Roberto Motterlini

► **To cite this version:**

Claire Douat, Pablo Escot Bocanegra, Sébastien Dozias, Robert Eric, Roberto Motterlini. Interaction of plasma generated carbon monoxide (CO) with mouse blood hemoglobin. 8th International Conference on Plasma Medicine, Aug 2021, Incheon (on line), South Korea. hal-03364149

**HAL Id: hal-03364149**

**<https://hal.science/hal-03364149>**

Submitted on 5 Oct 2021

**HAL** is a multi-disciplinary open access archive for the deposit and dissemination of scientific research documents, whether they are published or not. The documents may come from teaching and research institutions in France or abroad, or from public or private research centers.

L'archive ouverte pluridisciplinaire **HAL**, est destinée au dépôt et à la diffusion de documents scientifiques de niveau recherche, publiés ou non, émanant des établissements d'enseignement et de recherche français ou étrangers, des laboratoires publics ou privés.

**Journal:** Plasma Processes and Polymers

**Article type:** full paper

## **Production of carbon monoxide (CO) from He/CO<sub>2</sub> plasma jet as a new strategy for therapeutic applications**

Claire Douat<sup>1\*</sup>, Pablo Escot Bocanegra<sup>1</sup>, Sébastien Dozias<sup>1</sup>, Éric Robert<sup>1</sup>, Roberto Motterlini<sup>2</sup>

---

<sup>1</sup>GREMI UMR7344 CNRS, Université d'Orléans, Orléans, France

<sup>2</sup> University Paris Est, INSERM U955, IMRB, F-94010 Créteil, France

\*Correspondence

Claire Douat, GREMI UMR7344 CNRS, Université d'Orléans, France

Email: [claire.douat@univ-orleans.fr](mailto:claire.douat@univ-orleans.fr)

---

### **Abstract:**

A new method to deliver carbon monoxide (CO) for medical applications is presented using a kHz-driven helium plasma jet with 1% CO<sub>2</sub> admixture. Despite being known for its anti-inflammatory, vasorelaxing and anti-apoptotic effects, a possible role of CO generated from plasma for treating various diseases has so far been neglected.

Here we show that CO production of a plasma jet can be tuned from 100 to 2000 ppm. The number of CO molecules produced per pulse is in the range of  $1 \times 10^{12}$ – $1.5 \times 10^{13}$  range.

To assess the delivery of CO, mouse blood hemoglobin was used as scavenger of CO and the consequent formation of carboxyhemoglobin (COHb) was quantified. This study reveals for the first time that plasma can generate and deliver CO for therapeutic interventions.

### **Keywords:**

carbon monoxide ; CO<sub>2</sub> dissociation ; hemoglobin ; plasma jet ; plasma medicine ;

### **Abbreviations:**

[CO]<sub>measured</sub>, Concentration of CO measured with the gas analyzer

**[CO]<sub>plasma</sub>**, Concentration of CO produced in the plasma  
**C<sub>lis</sub>**, capacitance of the capacitor for the Lissajous measurement  
**CO-RMs**, CO-releasing molecules  
**COHb**, carboxyhemoglobin  
**d**, travel distance of species between two pulses  
**DBD**, Dielectric Barrier Discharge  
**EEDF**, Electron Energy Distribution Function  
**E<sub>pulse</sub>**, injected energy per pulse  
**f**, frequency of the applied voltage  
**l**, length of the plasma in the Teflon® tube  
**n**, number of sections along the plasma in the tube  
**N<sub>CO/pulse</sub>**, the number of CO produced per pulse  
**N<sub>0</sub>**, number of CO molecules produced per pulse  
**[O<sub>2</sub>]<sub>measured</sub>**, concentration of O<sub>2</sub> measured with the gas analyzer  
**P<sub>In</sub>** : power input  
**ppm**, parts-per-million  
**Q**, transferred charges  
**S**, section of the tube (the inner diameter was 4 mm)  
**sccm**, standard cubic centimeter per minute  
**SEI, E<sub>spec</sub>**, Specific Energy Input  
**v**, gas velocity  
**V<sub>d</sub>**, volume section of the plasma in the tube  
**V<sub>tot</sub>**, applied voltage  
**φ**, the total flow rate  
**φ**, gas flow rate

## 1 INTRODUCTION

Non equilibrium plasma has the ability to generate large population densities of reactive species, while keeping the overall gas temperature near room temperature allowing the plasma to be in contact with living tissues with no risk of burning. This singular feature led to the development of a new area, called *Plasma Medicine*. Research is now performed on many different topics including works on cancer treatment, wound healing, blood coagulation,

dentistry, cosmetology, sterilization and decontamination, among others.<sup>[1-10]</sup> The successes of plasmas have come so far from their versatility and their capacity to generate large amounts of reactive species combined with electric field, photons (IR, visible and UV) and charged particles.<sup>[11-16]</sup> A great number of the species are reactive oxygen and nitrogen species (RONS), such as atomic oxygen, ozone (O<sub>3</sub>), nitric oxide (NO) and hydroxyl (OH), produced by the interaction of the plasma with air. These RONS are known to have various beneficial effects such as antibacterial and vasodilator properties.<sup>[17]</sup> In particular, NO is widely studied in the field of *Plasma Medicine*, due to its ubiquitous role as signaling mediator and “gasotransmitter”.<sup>[18]</sup> Another important signaling molecule produced in mammalian cells is carbon monoxide (CO). Despite having a bad reputation due to the potentially lethal consequences when inhaled at high concentrations, low doses of CO appears to have many beneficial effects for human health and has a broad spectrum of biological activities such as anti-inflammatory, vasodilatory, anti-apoptotic and anti-proliferative effects.<sup>[19-23]</sup> It has been demonstrated in multiple preclinical models of disease that CO can be used in various applications such as organ transplantation and preservation, tissue ischemia, inflammatory and metabolic disorders.<sup>[20, 22, 24]</sup> Surprisingly, a potential role of CO generated by plasma jet to treat pathological disorders has been so far totally neglected.

Today, the two main systems used to deliver CO in medicine are CO inhalation and CO-releasing molecules (CO-RMs). Inhalation of small amounts of CO gas, from 100 to 1000 ppm, has already proved its efficiency in medicine and has been used for clinical applications.<sup>[24, 25]</sup> However, this technique is not easy to handle because of the difficulty in controlling the delivery of gaseous CO without causing systemic toxicity.<sup>[26]</sup> Furthermore, the delivery is not local and affects the whole human body via its binding to hemoglobin and transport in the blood. To overcome these issues, Motterlini *et al.* first addressed the use of CO-releasing molecules (CO-RMs) as potential therapeutic agents for the delivery of controlled amounts of CO and investigated the pharmacological effects of the first class of

these compounds.<sup>[27]</sup> The compounds have shown promising pharmacological effects in a variety of *in vivo* animal models,<sup>[20, 22]</sup> thus indicating that this strategic approach forms the basis for developing future formulations of a “solid form of CO” that can be delivered effectively for therapeutic applications.

As a possible alternative to CO-RMs could be the use of plasma. The latter can produce CO via dissociation of CO<sub>2</sub>, as it has been demonstrated in the CO<sub>2</sub> laser field and in energy storage field where the reduction of CO<sub>2</sub> to CO is an important step to store energy in the chemical bonds of hydrocarbons.<sup>[28, 29]</sup> Many studies devoted to this reaction revealed that, depending on the plasma source, the amount of CO can be tuned in a very broad range from less than few ppm to hundreds thousands ppm.<sup>[30]</sup>

In the present study, we propose to use a plasma fed with helium with small admixture of CO<sub>2</sub>, to produce CO at low doses for medical use. The new type of CO source has the advantage to produce CO locally and to combine the beneficial biological effects of CO and plasma in a same device. In this work, we characterized the plasma jet to find safe conditions for biomedical applications. The concentration of CO has been measured by means of a gas analyzer and the energy consumption via a Lissajous method. To assess and quantify the delivery of CO from plasma to liquid, we developed a system whereby mouse blood hemoglobin, a strong scavenger of CO, interacted with the plasma reaction. Once CO binds to hemoglobin, it forms carboxyhemoglobin (COHb), which can be precisely quantified by light absorption. We report here that controlled production of CO from plasma jet is feasible and could be engineered for therapeutic applications in the field of plasma medicine.

## **2 EXPERIMENTAL SECTION**

### **2.1 Plasma discharge**

The source of CO was a plasma jet from a reactor system, which is depicted in Figure 1, and was similar to the one used by Darny *et al.*<sup>[15]</sup> Plasma was generated in a dielectric capillary

tube with a 4 mm inner diameter and a 6 mm outer diameter. A ring electrode connected to the high voltage was inserted in the dielectric tube, while a grounded ring electrode wrapped the tube. The device was powered with a positive microsecond-duration voltage pulses from 2 to 15 kV with a frequency between 1 to 20 kHz, produced by a homemade power supply. Helium (99.999 % purity) gas mixed with 1% CO<sub>2</sub> (99.999 % purity) was flown through a high voltage electrode in 100–2000 standard cubic centimeter per minute (sccm) range, regulated by calibrated mass flow controllers.

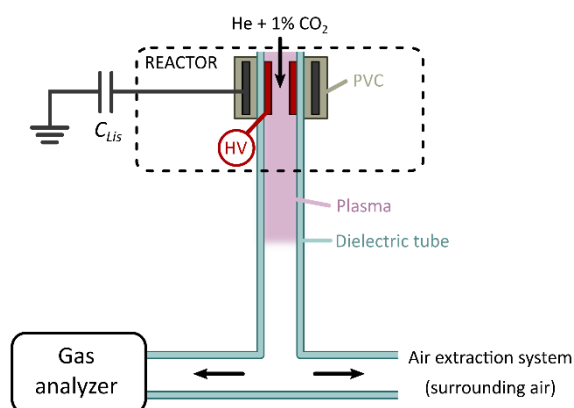


Figure 1: Schematic of the plasma jet reactor in indirect treatment configuration to measure the CO concentration with the gas analyzer.

Three configurations have been tested in this study: indirect treatment, direct treatment with grounded plate and direct treatment with grounded liquid. Their schematic representation is reported in Figure 2. In the case of indirect treatment, plasma was not in direct contact with the liquid. This means that the only plasma components which interacted with the target were the long-lifetime species. In direct treatment, plasma was in contact with the liquid, meaning that all the plasma components interacted with the target (electric field, charged particles, reactive species and light). There were two different configurations for the direct treatment: when the well lies on a grounded plate and when the liquid was directly connected to the ground. The dielectric tube was in glass and 10 cm long. As reported by Busco *et al*, the end of the tube was tapered with a 1.5 mm inner diameter and a 3 mm outer diameter as shown in

Figure 2.<sup>[31]</sup> In the case of indirect treatment, the dielectric tube was a 50 cm long Teflon® capillary tube connected to the same tapered glass tube used in direct treatment. We used Teflon® tubing as it is flexible and commonly used in the medical industry. For the three configurations the tube was immersed in 2 mm deep in the liquid.

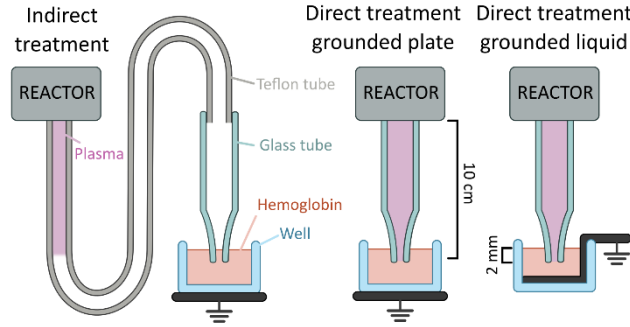


Figure 2: Schematic representation of the three configurations tested in this study.

## 2.2 Lissajous measurements

As the two electrodes were separated by a glass tube, the plasma jet reactor was here a dielectric barrier discharge (DBD). The power dissipated per cycle can be measured via a Lissajous method.<sup>[32]</sup> Initially this method was used for sinusoidal voltage, but it has been shown that this method was also valid for pulsed voltage.<sup>[33, 34]</sup> In this case the area of the Lissajous figure represents the energy dissipated in the discharge per pulse.

Transferred charges were collected on a capacitor ( $C_{lis} = 1.5 \text{ nF}$ ) to obtain the power dissipated in the discharge. The area of the loop formed by the transferred charges,  $Q$ , as a function of the applied voltage,  $V_{tot}$ , was proportional to the injected energy per pulse,  $E_{pulse}$ , and thus to the power input as well (*ie*, the power absorbed by the discharge) by this relation:

$P_{In} = f \cdot E_{pulse}$ , where  $f$  is the frequency of the applied voltage. The applied voltage and the

Lissajous voltages were respectively measured with a Tektronix P6015A probe (75 MHz, and 1000:1 division ratio) and with a Tektronix TPP050B probe (500 MHz and 10:1 division ratio). The signals were recorded with a 500 MHz bandwidth digital oscilloscope (Tektronix MDO3054). The overall shape of the applied voltage waveform was independent of the

maximum value of the applied voltage and pulse frequency. From 2 kV up to 15 kV, the voltage rise times (defined between 10% and 90% of the maximum values) and the full width at half maximum (FWHM) were almost constant, being equal to  $840 \pm 10$  ns and  $1.5 \mu$ s respectively.

### 2.3 Gas analyzer

As schematically represented in Figure 1, concentrations of exhaust gases of the plasma reactor such as  $\text{NO}_x$ , CO,  $\text{CO}_2$ , and  $\text{O}_2$  were measured continuously with a multi-gas analyzer (Kigaz 500 KIMO) in the indirect treatment configuration (cf Figure 2). The measuring range and accuracy of measurements as stated by the manufacturer were: 0 – 4000 ppm and 10 ppm for CO concentration, and 0 – 100 % and 0.2% for  $\text{O}_2$  concentration. Measuring the concentration of gases was not possible in a direct treatment because of the mixing with plasma and the surrounding air and liquid.

The analyzer required to pump the exhaust gas to take a sample. In our conditions the pumping rate of the analyzer was equivalent to 1500 sccm. In this study, the gas going through the plasma reactor was in the 100-2000 sccm range, meaning that for values lower than 1500 sccm, the gas sample was not only from the plasma but also from the air extraction system, where the gas was composed of the surrounding air. The plasma can produce a very small amount of  $\text{O}_2$  from the  $\text{CO}_2$  dissociation, but in our case this amount cannot be higher than 0.1%, since the maximum of CO concentration measured in our conditions was 2000 ppm. In a first approximation, we assume that there was no  $\text{O}_2$  in % range produced by the plasma. Thus, the  $\text{O}_2$  concentration,  $[\text{O}_2]_{\text{measured}}$ , gives an information on the ratio of the gas from the plasma and from the surrounding air measured by the analyzer. Thanks to this ratio, the CO concentration measured,  $[\text{CO}]_{\text{measured}}$ , with the analyzer can be corrected in order to know the right concentration,  $[\text{CO}]_{\text{plasma}}$ , in the plasma, and is expressed as:

$$[\text{CO}]_{\text{plama}}(\text{ppm}) = \frac{[\text{CO}]_{\text{measured}}(\text{ppm})}{21 - [\text{O}_2]_{\text{measured}}(\%) } \times 21 \quad (1)$$

The precision of the analyzer was 10 ppm and 0.2% for CO and O<sub>2</sub> concentration, respectively. Thus, the error of [CO]<sub>plasma</sub> was estimated with the uncertainty propagation calculation. Calibration of this method were performed using a gas mixture containing 1000 ppm of CO, and we measured a systematic error of 150 ppm.

In a gas phase, CO is a very stable molecule if the temperature does not exceed 3000 K,<sup>[30]</sup> which was our case since the measured gas temperature was always lower than 100 °C. The gas temperature in plasma was evaluated with a fiber optic temperature sensor (Optocon Fotemp). Additionally, the direct recombination of CO and O atom to CO<sub>2</sub> is spin forbidden. It means that it occurs very slowly with non-catalytic surfaces, which was the case here since the CO concentration was not influenced by the time of flight of the gas.<sup>[35, 36]</sup> Then, we can assume that loss processes are negligible in the present study.

It has to be noted that for all conditions tested in this study, neither NO nor NO<sub>x</sub> were detected, meaning that the concentration was lower than 5 ppm in the detector, but could be higher in the plasma since there are reactive species. During all experiments, no carbon deposits have been observed on the dielectric surface of the tube, even after several hours of operation. We also recorded the spectra of the plasma in 300 – 1100 nm range (data not shown), and no CO or C<sub>2</sub> bands were measured. The absence of CO band may be correlated with the relatively lower conversion rates in the present study.

#### **2.4 Detection of CO in blood plasma**

To assess and quantify the production of CO from plasma, we developed a system whereby hemoglobin, a strong scavenger of CO, was freshly collected from mice and then interacted with the plasma. Hemoglobin is the iron-containing oxygen-transport metalloprotein in red blood cells. The affinity of hemoglobin for CO is approximately 200 fold higher than the affinity for O<sub>2</sub> and once CO is bound to the heme it forms a very stable carboxyhemoglobin

(COHb).<sup>[37]</sup> The level of COHb was measured in mouse blood by light absorption after plasma treatment using a method previously described,<sup>[38]</sup> and then adapted by Nikam *et al.*<sup>[39]</sup> 120  $\mu$ L of blood were collected from a mouse and added to 57.6 mL of a buffer solution (tris(hydroxymethyl) aminomethane solution deoxygenated with sodium dithionite) corresponding to  $9 \pm 1$  mM of heme, and spectra were recorded after plasma treatment (direct and indirect treatment were tested) of this solution.

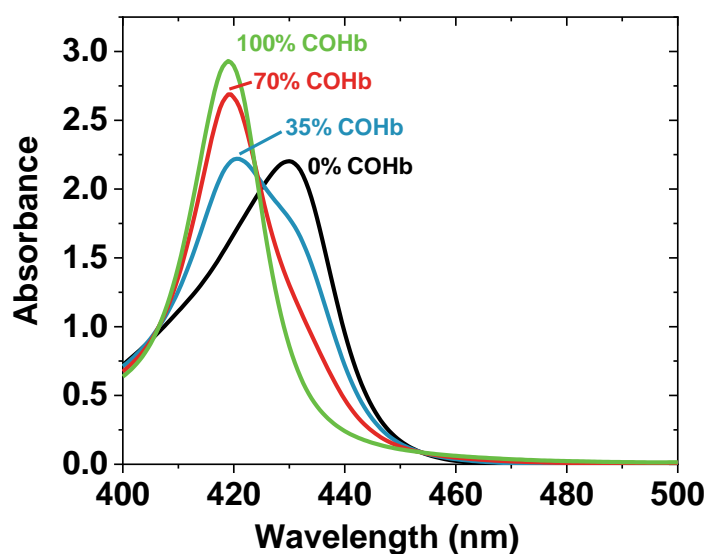


Figure 3: Absorption spectra before (black) and after the addition of 2500 ppm CO diluted in helium gas at a flow rate of 100 sccm with different treatment times (blue: 15 s, red: 30 s, green: 60 s).

In Figure 3, examples of absorption spectra are reported before (black) and after the addition of 2500 ppm CO diluted in helium gas at a flow rate of 100 sccm at different times of treatment: 15 s (blue), 30 s (red) and 60 s (green). For a similar absorption, the comparison of the absorption profile with the ones obtained with plasma treatment showed there was no difference, which ensured that the only species which bound to hemoglobin was the CO molecule. Figure 4 shows an example with 100% of COHb in various conditions: with a CO-releasing molecule (CORM-401) (blue), after 3 minutes of 2500 ppm CO diluted in helium gas at a flow rate of 100 sccm (red), and after 3 minutes of an indirect plasma treatment at 100

sccm of He with 1% of CO<sub>2</sub> at 20 kHz and 10 kV (green). For the direct plasma treatment, 100% of COHb was never reached, but the comparison of the absorption spectra with CORM and diluted CO gas at lower COHb value showed that the spectra were also identical.

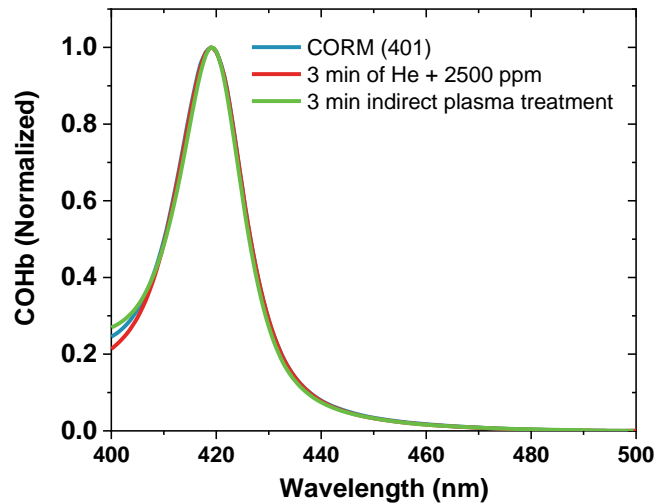


Figure 4: Comparison of the absorption spectra with 100% COHb with CORM-401 (blue), after 3 minutes of 2500 ppm CO diluted in helium gas at a flow rate of 100 sccm (red), and after 3 minutes of an indirect plasma treatment at 100 sccm of He with 1% of CO<sub>2</sub> at 20 kHz and 10 kV (green).

The percentage of COHb was calculated based on the absorbance at 420 and 432 nm, with the reported extinction coefficients for mouse blood hemoglobin [38]. One mL of this solution was placed in a 24-well plate, and for each configuration (direct and indirect treatment) the end of the dielectric tube of the reactor was immersed in 2 mm deep in the liquid (cf Figure 2). For the treatment of hemoglobin with plasma, we chose a gas flow rate of 100 sccm which produced a gentle bubbling in the liquid. Higher gas flows were not possible, since the bubbling was too important, and a part of the liquid was lost because of sputtering.

The maximum treatment time was 3 minutes, since longer time induced damages to hemoglobin. These damages may possibly be due to: 1) the liquid temperature which was higher than 42°C after 3 minutes; 2) a changes in pH, which was lower than 4; or 3) a gradual oxidation of hemoglobin over time. The error margin of the COHb measured with this method was estimated to be from 5% to 15%.

## 3 RESULTS AND DISCUSSION

### 3.1 Measure of CO

All the measurements presented in this section were by using the indirect configuration (cf Figure 2).

#### 3.1.1. Effect of the total gas flow

To estimate the effect of the total gas flow on the CO production by plasma jet, the relation between the CO concentration measured from the exhaust of the plasma and the gas flow rate was evaluated. The results are presented in Figure 5 in helium gas with 1% CO<sub>2</sub> admixture, a frequency of 20 kHz and an applied voltage of 10 kV. The graph shows that the concentration of CO (in blue) decreases as a function of the gas flow rate. At low flow rates, little amounts of gas from plasma exhaust were sampled in the gas analyzer, thus explaining why the uncertainties are bigger.

The right scale of Figure 5 presents the conversion degree, which is the ratio of the final CO density over the initial CO<sub>2</sub> density, and reaches the maximum of 15% at 100 sccm. The decrease of CO concentration as a function of gas flow can be explained by the residence time. The latter decreases with gas flow, and consequently, for similar energy injected per pulse and shorter residence time, the average energy spent on each CO<sub>2</sub> molecules decreases. Similar behaviors were observed for DBD in pure CO<sub>2</sub>.<sup>[40, 41]</sup>

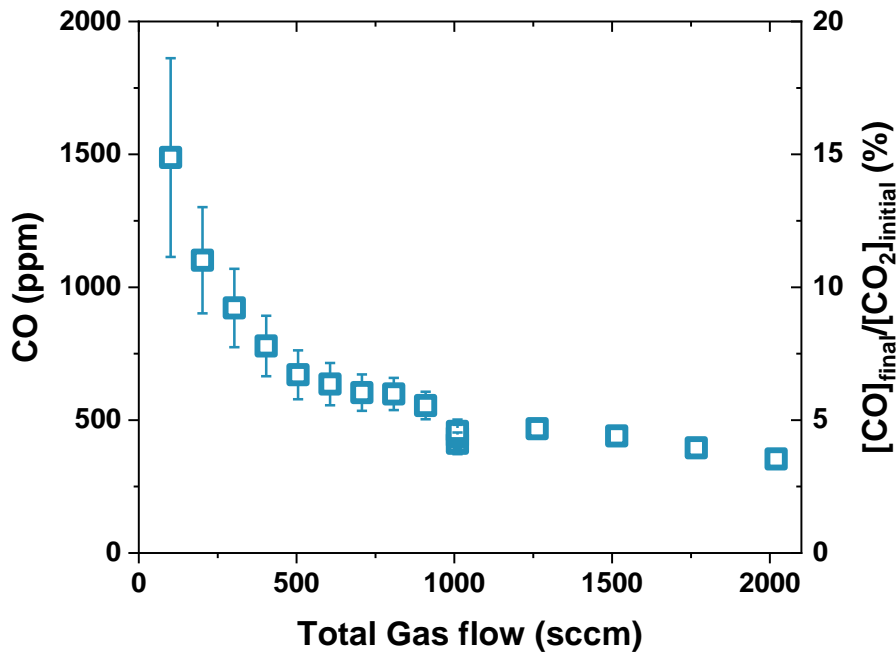


Figure 5: CO concentration (open blue square) and conversion degree versus the total flow rate in helium with 1% CO<sub>2</sub> admixture, with a frequency of 20kHz at 10kV.

### 3.1.2. Effect of discharge frequency

The frequency is a parameter affecting the concentration of CO. Figure 6 shows the influence of the frequency on CO concentration. As shown, the concentration increases linearly with the frequency up to 10 kHz before reaching a plateau at around 400 ppm. The linear part of this trend is easily explainable. As the injected energy per pulse,  $E_{pulse}$ , is independent of frequency, and rose  $26.3 \pm 0.7 \mu\text{J}$ , the total energy injected is proportional to the number of pulses and therefore to the frequency. The higher the energy, the higher CO concentration is until stabilization. But surprisingly, above 10 kHz, even if the injected energy per pulse remains constant, the concentration does not increase, and remains stable at 400 ppm.

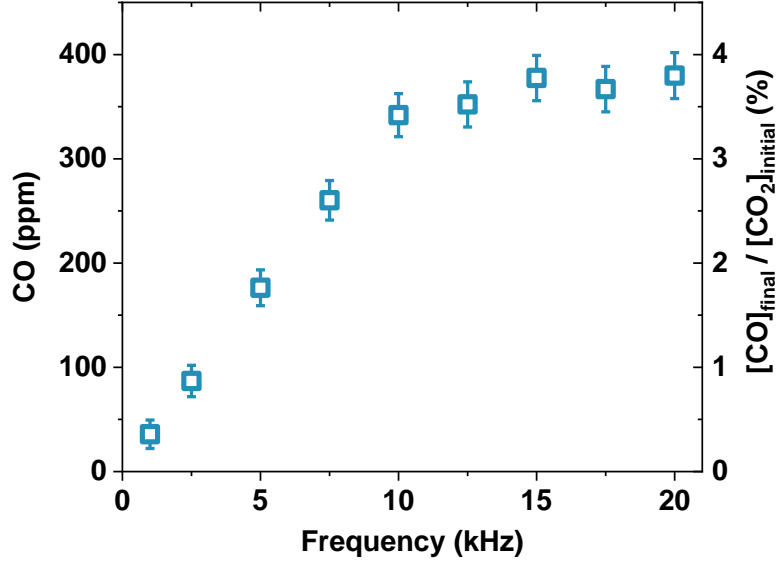


Figure 6: CO concentration versus the discharge frequency at 10 kV in helium with 1% CO<sub>2</sub> admixture with 1010 sccm as flow rate. The energy per cycle rose to  $26.3 \pm 0.7 \mu\text{J}$ .

In order to get more insights on the effect of the frequency on CO production, we estimated the number of CO produced per pulse. This parameter could also provide useful data for numerical models. It has to be noted, that in our conditions, the plasma propagated in the tube on around 25 cm long, and the frequency did not influence this length. To make the calculations easier, we split into sections the plasma in the tube like schematically represented in Figure 7, where  $l$  is the length of the plasma in the Teflon® tube,  $S$  is the section of the tube (the inner diameter was 4 mm), and  $d$  is the travel distance of species between two pulses.

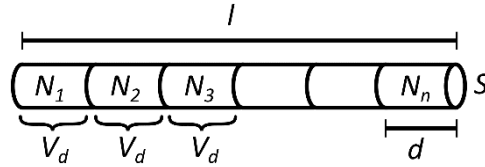


Figure 7: Schema of the plasma to calculate the number of CO produced per pulse.

We assume that in each small volume  $V_d$ , the number of CO molecules produced per pulse,  $N_0$ , is constant. The length of the plasma,  $l$ , is composed of  $n$  sections, and consequently, the number of CO produced per pulse is expressed as

$$N_{CO/pulse} = N_0 \times n \quad (2)$$

The first volume,  $V_d$ , saw one pulse, meaning that the number of CO molecules is equal to  $N_0$ . The second volume, saw two pulses, meaning that the number of CO molecules is equal to twice  $N_0$ , and etc. Therefore, we can generalize for the volume number  $n$ .

$$\begin{aligned}
 N_1 &= N_0 \times 1 \\
 N_2 &= N_0 \times 2 \\
 N_3 &= N_0 \times 3 \\
 &\dots \\
 N_n &= N_0 \times n
 \end{aligned} \tag{3}$$

The measured concentration with the gas analyzer,  $[CO]_{plasma}$ , corresponds to the concentration in the last section volume, and is expressed as

$$[CO]_{plasma} = \frac{N_n}{V_d} = \frac{n \times N_0}{S \times d} \tag{4}$$

As  $d$  is the travel distance of the species between two pulses, it can be expressed as

$$d = \frac{v}{f} = \frac{\phi}{S \times f} \tag{5}$$

Where  $v$  is the gas velocity,  $\phi$  the gas flow rate and  $f$  the frequency. By combining equations (2), (3), (4) and (5), we find

$$N_{CO/pulse} = \frac{[CO]_{plasma} \times \phi}{f} \tag{6}$$

Finally, the equation does not depend on the volume of the plasma, and the number of CO molecules produced per pulse depends only on the gas flow, the frequency and the CO concentration. This number is plotted in Figure 8, and is constant from 1 to 10 kHz. Its value is in the  $1.1 \times 10^{13} - 1.2 \times 10^{13}$  CO molecules range. Above 10 kHz, as expected, this number decreases linearly.

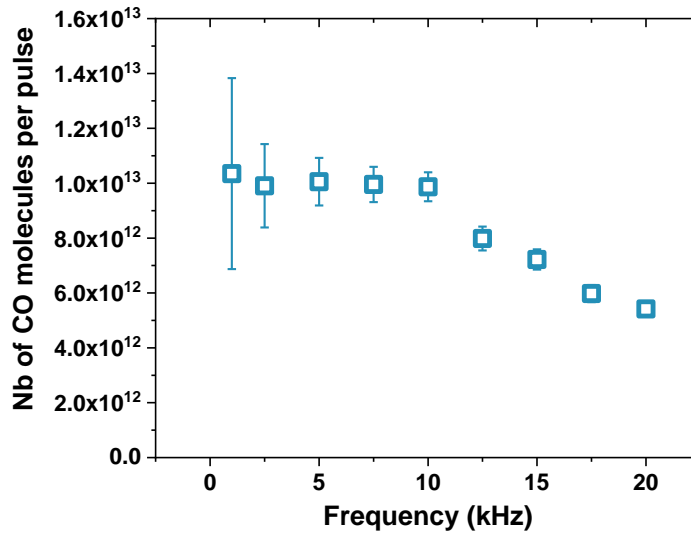


Figure 8: Number of CO molecules produced per pulse versus the frequency at 10 kV in helium with 1% CO<sub>2</sub> admixture with 1010 sccm as flow rate.

In this paper, the concentration of CO as a function of the frequency remains constant when the frequency is higher than 10 kHz, meaning that the number of CO molecules produced per pulse decreases. Further investigations were then carried to explore the potential reason of the decrease of this number. Potential reasons could be (1) the gas composition, (2) the accumulation of residual charges and (3) a modification of the chemistry.

### 3.1.2.1. Gas composition

The gas flow was 1010 sccm, meaning the gas velocity in a 4 mm diameter tube was 1.34 m/s. Thus, between two pulses, the species travel from 70 to 1300  $\mu\text{m}$  in the 1-20 kHz range. As the length of the plasma was a couple of decimeters, we can conclude there was an accumulation effect, and the gas composition along the length of the plasma was different. This difference may have an effect on CO production.

Initially, there are two species: He et CO<sub>2</sub> (we neglect impurities). Once plasma is on, it can produce various by-products, such as CO, C, O, O<sub>2</sub> and O<sub>3</sub>, just to name a few. The presence of these by-products may induce a change in the ionization coefficient and the electron energy

function distribution (EEDF), and thus decreases the production of CO per pulse when the accumulation effect is too important.

The most efficient process to dissociate CO<sub>2</sub> is by vibrational up-pumping along the asymmetric mode <sup>[30]</sup>. Aerts *et al* showed that in a DBD configuration, this channel is significant if there is an accumulation effect <sup>[42]</sup>. If the inter-pulse time exceeds 10 μs, most of the vibrationally excited CO<sub>2</sub> molecules relax back to the ground state, and the dissociation by vibrational up-pumping is insignificant. Ponduri *et al* showed that the generation of CO mainly takes place during the discharge pulses, meaning when the plasma occur <sup>[35]</sup>. In our case, since the frequency is in the 1-20 kHz range, the inter-pulse time is in the 50-1000 μs range, which is definitively too long to have an accumulation effect. We can conclude that the dissociation of CO<sub>2</sub> by vibrational up-pumping is insignificant here, and that CO molecules are mainly produced by electron impact dissociation or by collision with helium excited atoms.

The dissociation of CO<sub>2</sub> in CO by direct electronic impact requires electrons with a minimum energy of 7 eV.<sup>[30]</sup> Here, CO can also be produced by collision with helium excited atoms, where the lowest levels are at around 20 eV.<sup>[43]</sup> Among these excited states, He metastable atoms act as energy reservoir in plasma jet.<sup>[12]</sup> These two reactions are the two main probable production reactions in He/CO<sub>2</sub> plasma jet,<sup>[43]</sup> and require energetic electrons. Sretenović *et al* showed that electron density in a streamer head in a capillary of a helium plasma jet, which is our case here, is related to the electric field strength in the streamer head <sup>[44]</sup>. As the Townsend ionization coefficient depends on the local electric field, the evolution of the electron density can be estimated from this coefficient. In Figure 9, we determined the effective ionization coefficient, which is the subtraction of the ionization coefficient from the attachment coefficient, for various gas mixtures by using the freeware solver BOLSIG+ (version 2019).<sup>[45]</sup> The Boltzmann equation was solved by using the Phelps collision cross-section database.<sup>[46]</sup> Here, the gas temperature was in the range of 310 to 360 K, and for the

calculation we choose 330 K. The results are presented in Figure 9. It has to be noted that this calculation is indicative, since it does not take into account the impurities that plays a role in Penning ionization with He\* .

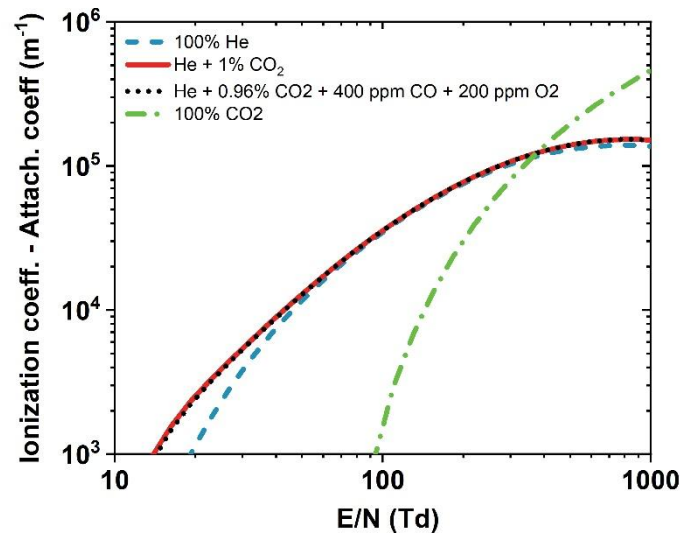


Figure 9: Townsend coefficient as a function of the reduced electric field for various gas mixtures at 330 K : pure helium (dash blue line); He/CO<sub>2</sub> 0.99/0.01 (red line), He/CO<sub>2</sub>/CO/O<sub>2</sub> 0.9898/0.0096/0.0004/0.0002 (dot black line) and pure CO<sub>2</sub> (dash dot green line).

The effective ionization coefficient at high reduced electric field does not depend on the gas mixture when the main gas is helium, but below 100 Td it becomes larger in helium with 1% admixture of CO<sub>2</sub> (red line) than in pure helium (dash blue line). As the ionization energy of CO<sub>2</sub> is 13.8 eV, excited atoms of helium, which have an energy higher than 19 eV, can ionize CO<sub>2</sub> molecules via Penning ionization. When the density of CO<sub>2</sub> remains low, this effect improves the ionization coefficient. But in pure CO<sub>2</sub> (dash dot green line), the effective ionization coefficient is lower than in helium, due to the molecular structure of this gas, which loses a part of the energy to populate the rotational and vibrational states instead to ionize. Once CO is produced, an O atom is formed. The latter can then be involved in other chemical reactions and produce others species such as O<sub>2</sub> or O<sub>3</sub>. In order to make the calculations simpler, we assumed that all O atoms were converted in O<sub>2</sub>. Meaning that the concentration of

O<sub>2</sub> molecules is two times smaller than CO. In our case, from 10 to 20 kHz (cf Figure 6), the concentration of CO was 400 ppm. If we assumed that that all O atoms were converted in O<sub>2</sub>, the O<sub>2</sub> concentration would have been 200 ppm, meaning that the gas composition was He/CO<sub>2</sub>/CO/O<sub>2</sub> 0.9898/0.0096/0.0004/0.0002. The ionization coefficient is plotted in Figure 9 (dot black line), and the latter is very close to the He with 1% CO<sub>2</sub> condition (red line). Thus, one could consider the small change in gas composition in our conditions does not affect the ionization coefficient, and consequently does not impact the electron density. Therefore, it does not explain why the number of CO produced per pulse decreases with the frequency from 10 kHz. We also calculated the electron energy distribution function (EEDF) for the gas mixture tested in Figure 9, and they were barely affected by the change of gas composition.

#### 3.1.2.1. Accumulation of residual charges

Nie *et al* showed the frequency of the applied voltage plays an important role on the seed electron density in jet plasma,<sup>[47]</sup> while Robert *et al* observed a significant decrease of plasma length from 1 to 75Hz, that may result from the inner capillary wall charging.<sup>[48]</sup> Wu *et al* found out that the length of the plasma plume for the very first discharge pulse is longer than for the following pulses, showing that even at low frequency, meaning in kHz range, the residual charges, such as positive ions, plays an essential role in the physic of plasma jet.<sup>[49]</sup> Mc Kay *et al* showed that in pulsed kHz plasma jet in helium, the concentration of positive ions remains high up to around 100 μs,<sup>[50]</sup> which is the time between two pulses at 10 kHz.

In our case, the powered electrode is in direct contact with the plasma. As this electrode is connected to a positive voltage pulse, it represents the anode. After the breakdown, the electrons seek into the anode, and positive charges remains. The number of these positive charges increases with the frequency, and if their number is high enough, it can modify the impact of the external electric field, and as a result the breakdown, the electron density and also the EEDF. This would have a direct impact on the number of CO produced per pulse. A

change in the breakdown voltage may also affect the propagation length of the plasma in the tube, but it was not what we observed in our case, meaning that if the accumulation of residual charges plays a role in the number of CO produced per pulse, it must be minor.

### 3.1.2.3. Modification of the chemistry

Studies on the production of ozone by non-thermal plasma show that the production of ozone can be alleviated by the production of nitrogen oxides and other species, which prevails over the production of ozone. Each oxygen atoms do not lead necessarily to the formation of one ozone molecule, when additional reactions involving oxygen atoms gain importance.<sup>[51]</sup> In a similar way the production of CO could be alleviated when the frequency increases. The accumulation effect increases with the frequency, meaning some of the species produced by the preceding pulse were still present during the following pulse. The accumulation of these species could induce a different chemistry and therefore a modification on the production of CO. The determination of the potential reactions in competition with the production reactions of CO would require a detailed study of the chemical reactions occurring in the plasma and its vicinity, which is beyond the scope of the present paper.

Thus, we can conclude that for a frequency higher than 10 kHz, the production of CO per pulse decreased. This could be due to an accumulation effect either by positive ions or by the chemical species or both. To fully understand this observation, further studies are needed. We will keep working on it and will present it in a dedicated paper in the future.

### 3.1.3. Effect of applied voltage

Figure 10 represents the effect of applied voltage on the concentration of CO molecules for various gas flow rates at 20 kHz. The error bars are bigger at low gas flow due to the fact that the amount of gas from plasma exhaust sampled by the analyzer was smaller than at higher gas flow rate. We can see that increasing the voltage leads to an increase in the concentration

of CO. Boeuf *et al* showed in their numerical model that in helium plasma jet, increasing the applied voltage induces a slight increase of the electric field.<sup>[52]</sup> The latter has a direct influence on the number of energetic electrons, which can contribute to the improvement of CO<sub>2</sub> conversion to CO.<sup>[40]</sup> But in our case, this increase is mainly explained with the energy dissipated in the discharge per pulse, since it increased with the applied voltage. For example, it went from around 10 μJ to 30 μJ, from 5 kV to 10 kV. The higher is the energy, higher the CO production is.

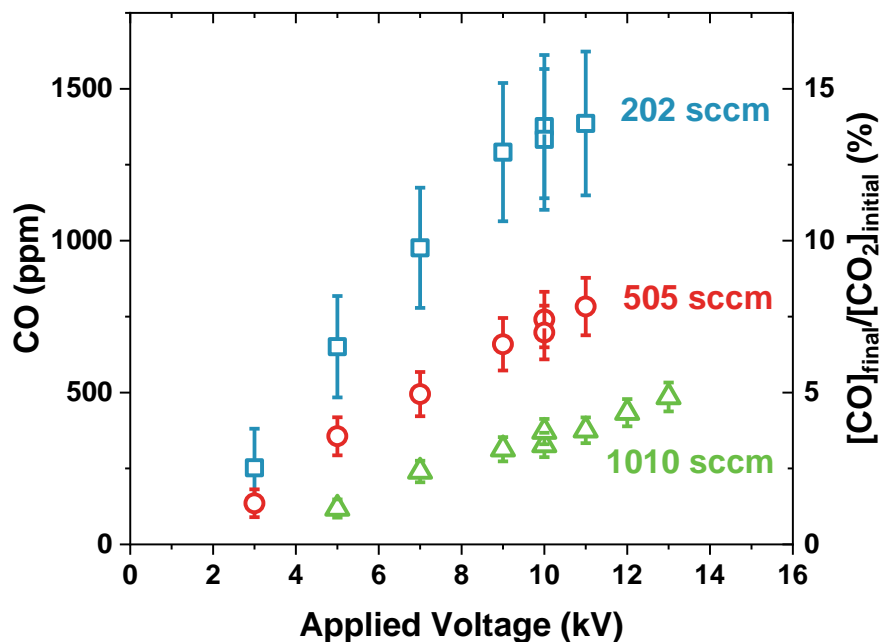


Figure 10: CO concentration versus the applied voltage at 20 kHz in He with 1% CO<sub>2</sub> admixture for various gas flows: 202 sccm (blue square), 505 sccm (red circle) and 1010 sccm (green triangle).

### 3.1.4. Specific energy input

The specific energy input (SEI) is an important metric to know the energy cost.<sup>[53]</sup> It is an intensive parameter, meaning that it does not depend on the system size. It represents the average amount of energy that is spent on each molecule of the gas. This parameter is defined as

$$E_{spec}(J/l) = SEI = \frac{P_{In}(W)}{\varphi(l/s)} \quad (6)$$

where  $P_{In}$  is the power input and  $\varphi$  the total flow rate. Note that the latter is expressed in standard conditions ( $T_0 = 273.15$  K,  $p_0 = 1013.25$  mbar).

The CO concentration and the conversion degree are plotted in log-log scale as a function of the SEI in Figure 11 for all the data presented in this paper. Condition details are written on the figure. We observe that the yield of CO increases with SEI. At a first glance, all the data follow the same trend, but if we look carefully, the trends of each set of data are slightly different. Previous works showed that in pure CO<sub>2</sub> DBD, the scaling parameter on CO<sub>2</sub> conversion was the SEI.<sup>[29, 35, 41, 54–57]</sup> But in our case, we cannot make this conclusion since the trends were slightly different for each condition. In pure CO<sub>2</sub> DBD, plasma remained in the electrode confinement, while it is not the case with a plasma jet, since the plasma length depends on various parameters. Although the SEI is an intensive parameter like the temperature, if the volume of the plasma varies, the absorbed energy by plasma would be different, which would induce a change in the SEI. This may explain why here the conversion degree is not a clear straight line as a function of the SEI.

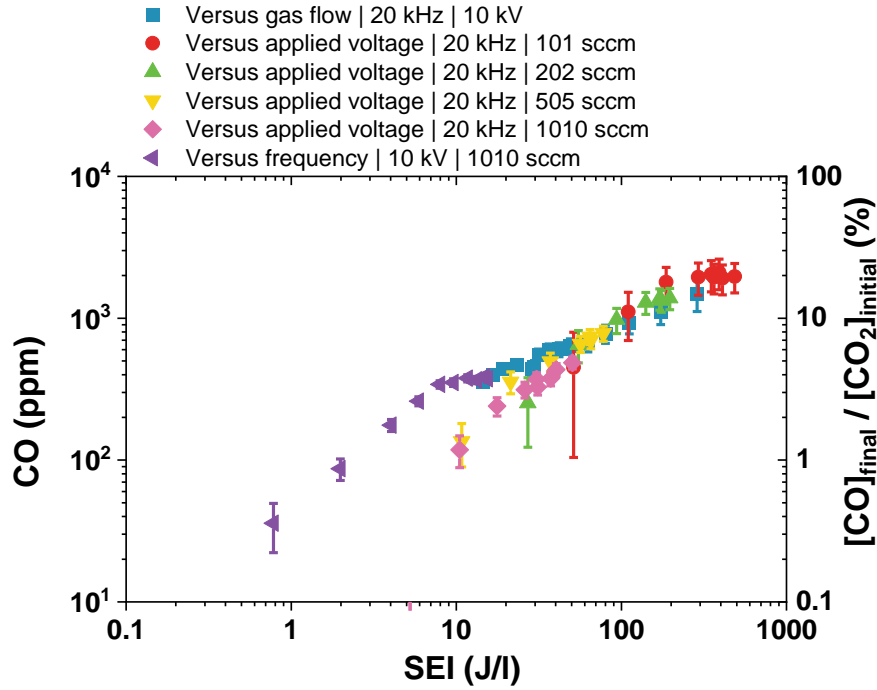


Figure 11: Conversion degree versus the specific energy input (SEI) for the all the data presented in the paper. Conditions: He with 1% CO<sub>2</sub> admixture.

The conversion degree is much higher with CO<sub>2</sub> diluted in helium than in pure CO<sub>2</sub>. For example, Brehmer *et al* measured at 1000 J/l a CO concentration at around  $5 \cdot 10^{16} \text{ cm}^{-3}$  in atmospheric pressure CO<sub>2</sub> DBD, which represents a CO<sub>2</sub> conversion of 0.2 %. If we extend the trend of Figure 11, we would get a conversion in the 30-50 % range, which is 100 time more<sup>[41]</sup>. Similar behavior has been observed by Ramakers *et al* in a DBD.<sup>[58]</sup> They measured that the CO<sub>2</sub> conversion drastically increased with the dilution of CO<sub>2</sub> in He. The lower CO<sub>2</sub> concentration they measured was at 5%, and they got 25% CO<sub>2</sub> conversion compared to 5% conversion in pure CO<sub>2</sub>. Urbanietz *et al* also measured the CO<sub>2</sub> conversion, but in RF driven plasma jet. They obtained better conversion degree at very low CO<sub>2</sub> fraction.<sup>[59]</sup> At 1% CO<sub>2</sub> admixture, the maximum conversion they measured was 15%. As He is an atomic gas, once ionized, the energy of electrons is not lost in gas heating by populating the rotational and vibrational levels. This advantage allows to get a larger EEDF with a large amount of energetic electrons. On the contrary, in a molecular gas, like CO<sub>2</sub>, most of the electron energy

is spent in gas heating inducing a lower electronic temperature. As a result, the ionization coefficient in helium is larger than in pure CO<sub>2</sub>, as shown in Figure 9. As discussed aforesaid, in DBD the CO<sub>2</sub> dissociation requires energetic electrons, which explains why the CO<sub>2</sub> conversion is more efficient when the CO<sub>2</sub> molecules are diluted in helium. In this work, as the dilution is important, the CO<sub>2</sub> conversion rose a maximum value of 15%. It has to be note, that even if the efficiency is better than in pure CO<sub>2</sub> DBD, it does not allow to produce large quantities of CO molecules.

#### 3.1.4. Plasma jet, a safe CO source

Finally, the CO concentration obtained with the plasma jet is from a couple of tens ppm to thousand ppm. CO is a toxic gas that binds to hemoglobin instead of O<sub>2</sub> and forms carboxyhemoglobin (COHb). In a previous paper, we explained that, to ensure safe conditions, the percentage of COHb in the blood has to be lower than 10%.<sup>[23]</sup> For example, the exposure time must not exceed 12 minutes for 1000 ppm. The maximum CO produced by the plasma jet was 2000 ppm, meaning that a treatment time of a couple of minutes is safe. In addition, if the jet propagates in air, the CO produced by the plasma would be diluted by the surrounding air, which will improve the safety of the treatment. We can conclude that the production of CO by the plasma jet remains in safe conditions. Moreover, this concentration can be tuned by varying the plasma parameter in order to get a concentration from a couple of tens ppm to a couples of thousands ppm, and this range is typically the one used in clinical applications for CO inhalation.<sup>[24, 25]</sup>

### 3.2 COHb

To study the effect of plasma, and specifically its production of CO on biomolecules, we developed a system whereby mouse blood hemoglobin, a strong scavenger of CO, interacted with the plasma. The formation of carboxyhemoglobin (COHb) was quantified by light

absorption (*cf* experimental section). In this section, the measurements were performed with a gas flow of 100 sccm of He with 1% CO<sub>2</sub> admixture, with an applied voltage of 10 kV and a frequency of 20 kHz. The three configurations presented in Figure 2 have been tested.

The quantity of COHb was first measured with no plasma, and with a gas flow of helium with controlled admixture of CO in order to calibrate the system. Figure 12 presents the percentage of COHb as a function of the time for four different CO concentrations: 250 ppm, 500 ppm, 1000 ppm and 2500 ppm. At 2500 ppm, the quantity of COHb increases linearly with the time to finally reach 100%. 100% means that all hemoglobin proteins are saturated with CO. The remained CO molecules were either dissolved in the liquid or degassed. The trends for the three other concentrations were also linear, but with a less important slope than for 2500 ppm.

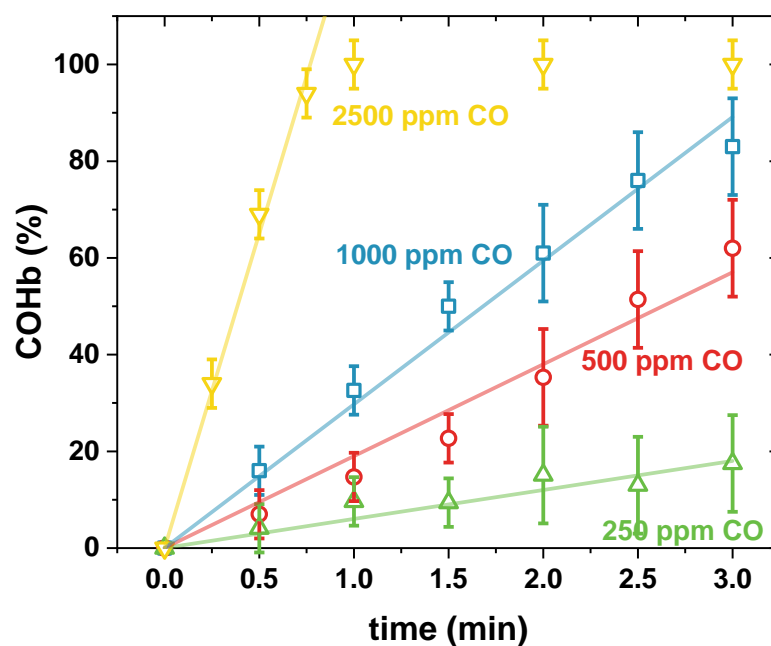


Figure 12: Percentage of COHb formation over time using various concentrations of CO diluted in helium: 250 ppm (green up-pointing triangle), 500 ppm (red circle), 1000 ppm (blue square) and 2500 ppm (yellow down-pointing triangle). Condition: 100 sccm.

Figure 13 presents the percentage of COHb over time for the three types of treatments presented in Figure 2: indirect treatment (blue square), direct treatment with a grounded

metallic plate under the well (red square) and direct treatment with the liquid grounded (green triangle). The percentage of COHb, for direct treatment when the liquid was grounded (green triangle), increases linearly with the time to reach 100% (by taking into account the error bars) after 2 minutes of treatment. The trends of direct treatment with the grounded plate (red circle) and the indirect treatment (blue square) are very similar, and increase linearly with time, reaching almost 90-100% after 2.5 minutes.

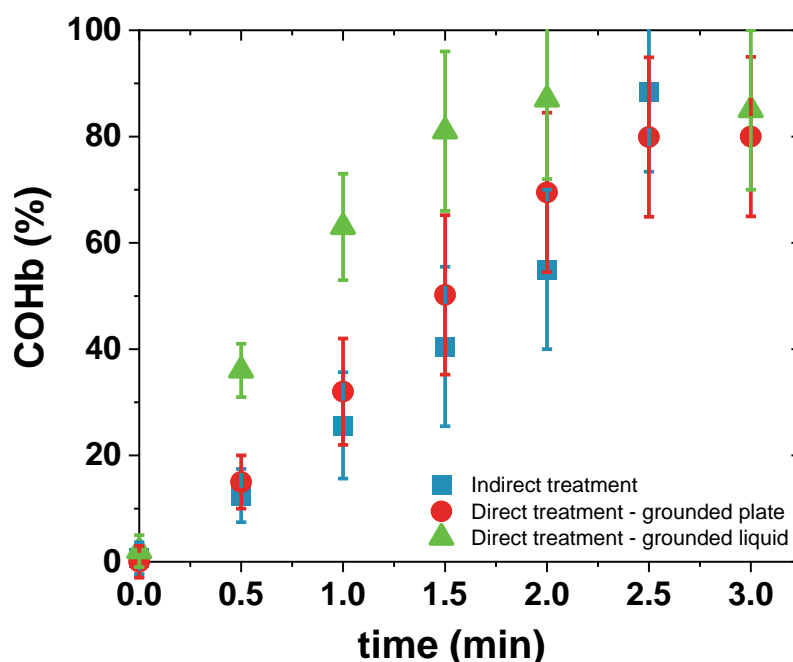


Figure 13: Percentage of COHb over time for the three different types of plasma treatments: indirect treatment (blue square), direct treatment with the plate grounded (red square) and direct treatment with the liquid grounded (green triangle). Condition: 100 sccm He with 1% CO<sub>2</sub> admixture, 20 kHz, 10 kV.

In order to evaluate the concentration of CO produced by plasma, we compared the results obtained with plasma (Figure 13) and with known concentrations of CO gas (Figure 12). We report in Figure 14 the value of the slopes of the linear part of the percentage of COHb formation over time for the calibrated gas at various concentrations of CO (cf Figure 12). We fit the data with a polynomial function and is represented by the dashed line. The slopes were also measured in plasma treatment, and were reported in Figure 14 to find the equivalence

with a calibrated gas treatment, and are represented by the blue, red and green rectangles. The width and the length of the rectangles represent the error margins. We found:

- Indirect treatment: [CO] = 850 – 1000 ppm
- Direct treatment – grounded plate: [CO] = 800 – 1000 ppm
- Direct treatment – grounded liquid: [CO] = 1500 – 1600 ppm

In the previous section, we measured the CO concentration in the exhaust of a plasma jet in an indirect configuration, and at 100 sccm we found a concentration of 1500 ppm  $\pm$  350 ppm. Compared to 850 – 1000 ppm, which is the concentration found from Figure 14, the difference is significant. This means that even if the CO concentration of plasma exhaust was 1500 ppm, this exhaust behaved on hemoglobin like a helium gas with 850-1000 ppm of CO. It means that plasma has an impact on CO binding. In indirect configuration, the only component that interact with the liquid is the long-lifetime species. In our case, the plasma does not produce only CO, but also others species such as O<sub>3</sub>, O<sub>2</sub> and C. This chemistry may impact the effects of CO on hemoglobin and avoiding the bonding with it. Even if the affinity of O<sub>2</sub> for hemoglobin is 200 fold lower than the affinity for CO,<sup>[37]</sup> this molecule can bind with it and modify the absorption spectra. To prevent O<sub>2</sub> binding, sodium dithionite solution was used. NO can also bind to hemoglobin with strong affinity,<sup>[60]</sup> and can be produced here by plasma with N<sub>2</sub> and O<sub>2</sub> that are always present in trace amounts. In the indirect configuration, in the exhaust of the plasma, the concentration of NO was estimated to be lower than 5 ppm. In direct treatment, the NO concentration has not been measured, but as the plasma interacted directly with the liquid, which interacted with air, the production of NO may be higher in this configuration. The spectra of NO-hemoglobin or O<sub>2</sub>-hemoglobin were different from COHb spectra (data not shown). As the comparison of the spectra with plasma was exactly the same with the absorption spectra with a CO-releasing molecule (CORM-401) (cf Figure 4), and very different from NO-releasing molecules or from no sodium dithionite

(meaning with O<sub>2</sub>) (data not shown), we ensured that the only specie which bound to hemoglobin was the CO molecule, and reinforces that no NO was produced in our conditions. Other chemical products, such as nitrite and nitrate, could modify the absorption profile, but in our case it is negligible since the profiles were identical with plasma, in CO diluted in helium gas and with CORM.

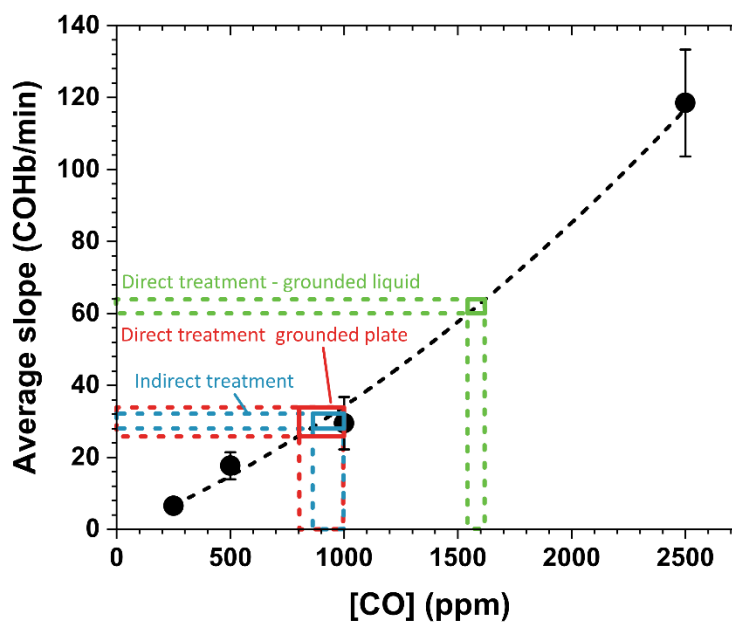


Figure 14: Value of the rising slope of Figure 12 versus the CO concentration diluted in helium for a gas flow of 100 sccm. The values of the slopes with plasma are reported on the graph.

Jablonowski *et al* investigated the solvation of NO, which is a gasotransmitter like CO, in a phosphate-buffered saline solution (PBS). They compared the NO concentration in the liquid with an argon gas with 40 ppm NO admixture and with an argon plasma. To reach a similar NO concentration in the liquid, the pure gas treatment had to be extended 20 fold of the plasma treatment time, while the NO concentration in the plasma was estimated to 8 ppm.<sup>[61]</sup> They showed that plasma improved the NO solvation in liquid. In our case, we observe the opposite effect with CO, since for a same concentration, a calibrated gas is more efficient. But those results were preliminary results, and more investigations are required to fully understand the impact of plasma on CO binding with hemoglobin. Future studies would

possibly allow to find conditions where plasma is even more efficient than a calibrated gas. Additionally, the comparison of a calibrated gas and plasma was only made for an indirect plasma treatment. However, the combination of all the plasma components (electric field, charge particles, light and reactive species) present in direct treatment could have also an impact on the interaction of CO with hemoglobin.

#### **4 CONCLUSION**

Carbon monoxide (CO) has a bad reputation due to the potentially lethal consequences when inhaled at high concentrations. However, in low quantities, it appears to have many beneficial effects for human health and has a broad spectrum of biological activities such as anti-inflammatory, vasodilator, anti-apoptotic, and anti-proliferative effects. It is a natural signaling molecule and plays a key regulatory role as second messenger in biological systems. It exhibits physiological functions similar to NO. Indeed, these two biomolecules are classified within the same category of “gasotransmitters”.

In this paper, we propose to use a plasma jet as a new CO source for medical use. We characterized a kHz-driven helium plasma jet with 1% CO<sub>2</sub> admixture to produce small amounts of CO in safe conditions for biomedical applications. The concentration of CO has been measured by means of a gas analyzer and the energy consumption via a Lissajous method. To assess and quantify the production of CO from plasma to liquid, we developed a system whereby mouse blood hemoglobin, a strong scavenger of CO, interacted with the plasma reaction. Once CO bound to hemoglobin, it formed carboxyhemoglobin (COHb), which was precisely quantified by light absorption. We reported here that controlled production of CO from plasma jet is feasible and could be engineered for therapeutic applications in the field of plasma medicine.

The plasma jet was a kHz DBD like reactor, meaning the dissociation of CO<sub>2</sub> by vibrational up-pumping was insignificant, and that CO molecules were mainly produced by electron

impact dissociation or by collision with helium excited atoms. This reactor was able to produce from a couple of tens ppm to thousand ppm of CO, which is typically the range used in clinical applications for CO inhalation, meaning it was safe and suitable for medical use. Moreover, this concentration could be tuned by varying the plasma parameters such as the gas flow rate, the applied voltage of the discharge frequency.

We showed that the CO concentration increased with the specific energy input, but was not the scaling parameter on CO<sub>2</sub> conversion like in pure CO<sub>2</sub> DBD, since it also depended on others parameters such as the gas flow rate, the applied voltage and the frequency. This may be due to the fact that, compared to classical DBD, the plasma produced by the jet propagated away from the confinement of electrodes, and its length propagation varied. Compared to pure CO<sub>2</sub> DBD, the conversion degree was higher. This was due to the fact that helium is an atomic gas, meaning that the energy of electrons was not lost in gas heating by populating the rotational and vibrational states, allowing to get a large amount of energetic electrons able to dissociate CO<sub>2</sub>.

The number of CO molecules produced per pulse was estimated, and we found, at 10 kV and for a frequency between 1-10 kHz, that this number was in the  $1.1 \times 10^{13}$ – $1.2 \times 10^{13}$  range, and decreased for higher frequency.

Finally, we showed that the quantity of CO molecules that bound to hemoglobin increased linearly with time. This study revealed for the first time that plasma influenced the binding of CO with hemoglobin, since this binding was better with CO diluted in helium gas than with CO produced by plasma (both conditions had the same CO concentration).

In summary, in this work we designed a new type of device for delivering CO for medical use. It allows to combine the beneficial biological effects of CO and plasma in a same device. It opens opportunities to develop new strategies for using therapeutic delivery of CO to treat a variety of disorders such as skin wound, cancer and blood coagulation, but also in other fields of biology such as cosmetics and agriculture.

## ACKNOWLEDGMENTS

This work was supported by GREMI laboratory (Orleans, France) through the internal project “COMA” and was performed in the framework CNRS GDR 2025 HAPPY BIO. CD wishes to thank Dr. Toufik Boushaki from ICARE (Orleans, France) for the loan of the gas analyzer.

## AUTHOR CONTRIBUTIONS

Conceptualization: C.D. | Design of the power supply: S.D. | Methodology: C.D., P.E.B. & R.M. | Data acquisition: C.D. & R.M. | Data interpretation: C.D. & R.M. | Writing original draft presentation: C.D. | Writing review and editing: C.D, E.R., P.E.B., R.M. All authors discussed the results, reviewed the manuscript, and have read and agreed to the published version of the manuscript.

## DATA AVAILABILITY STATEMENT

The data that support the findings of this study are available from the corresponding author upon reasonable request.

## REFERENCES

- [1] D. Yan, J. H. Sherman, and M. Keidar, *Oncotarget*, **2017**, 8 (9), 15977–15995.
- [2] D. B. Graves, *Plasma Process. Polym.*, **2014**, 11 (12), 1120–1127.
- [3] J. Heinlin, G. Isbary, W. Stolz, G. Morfill, M. Landthaler, T. Shimizu, B. Steffes, T. Nosenko, J. Zimmermann, and S. Karrer, *J. Eur. Acad. Dermatology Venereol.*, **2011**, 25 (1), 1–11.
- [4] M. G. Kong, G. Kroesen, G. Morfill, T. Nosenko, T. Shimizu, J. van Dijk, and J. L. Zimmermann, *New J. Phys.*, **2009**, 11 (11), 115012.
- [5] M. Laroussi, *IEEE Trans. Plasma Sci.*, **2009**, 37 (6), 714–725.
- [6] G. E. Morfill, M. G. Kong, and J. L. Zimmermann, *New J. Phys.*, **2009**, 11 (11), 115011.
- [7] T. H. Chung, A. Stancampiano, K. Sklias, K. Gazeli, F. M. André, S. Dozias, C. Douat, J. M. Pouvesle, J. S. Sousa, É. Robert, and L. M. Mir, *Cancers (Basel)*, **2020**, 12 (1).
- [8] M. Vandamme, E. Robert, S. Pesnel, E. Barbosa, S. Dozias, J. Sobilo, S. Lerondel, A.

- Le Pape, and J.-M. Pouvesle, *Plasma Process. Polym.*, **2010**, 7 (3–4), 264–273.
- [9] H. Tanaka, K. Ishikawa, M. Mizuno, S. Toyokuni, H. Kajiyama, F. Kikkawa, H.-R. Metelmann, and M. Hori, *Rev. Mod. Plasma Phys.*, **2017**, 1 (1), 3.
- [10] E. Stoffels, A. J. Flikweert, W. W. Stoffels, and G. M. W. Kroesen, *Plasma Sources Sci. Technol.*, **2002**, 11 (4), 383–388.
- [11] G. Cadot, C. Douat, V. Puech, and N. Sadeghi, *IEEE Trans. Plasma Sci.*, **2014**, 42 (10), 2446–2447.
- [12] C. Douat, I. Kacem, N. Sadeghi, G. Bauville, M. Fleury, and V. Puech, *J. Phys. D. Appl. Phys.*, **2016**, 49 (28), 285204.
- [13] C. Douat, S. Hübner, R. Engeln, and J. Benedikt, *Plasma Sources Sci. Technol.*, **2016**.
- [14] K.-D. Weltmann, H.-R. Metelmann, and T. von Woedtke, *Europhys. News*, **2016**, 47 (5–6), 39–42.
- [15] T. Darny, J.-M. Pouvesle, V. Puech, C. Douat, S. Dozias, and E. Robert, *Plasma Sources Sci. Technol.*, **2017**, 26 (4), 045008.
- [16] J.-M. Pouvesle, T. Darny, T. Maho, V. Puech, C. Douat, S. Dozias, and E. Robert, *Plasma Med.*, **2018**, 8 (1), 83–92.
- [17] D. B. Graves, *J. Phys. D. Appl. Phys.*, **2012**, 45 (26), 263001.
- [18] C. Szabo, *Sci. Transl. Med.*, **2010**, 2 (59), 59ps54-59ps54.
- [19] S. Minegishi, A. Yumura, H. Miyoshi, S. Negi, S. Taketani, R. Motterlini, R. Foresti, K. Kano, and H. Kitagishi, *J. Am. Chem. Soc.*, **2017**, 139 (16), 5984–5991.
- [20] R. Motterlini and R. Foresti, *Am. J. Physiol. Physiol.*, **2017**, 312 (3), C302–C313.
- [21] B. E. Mann and R. Motterlini, *Chem. Commun.*, **2007**, (41), 4197.
- [22] R. Motterlini and L. E. Otterbein, *Nat. Rev. Drug Discov.*, **2010**, 9 (9), 728–743.
- [23] E. Carbone and C. Douat, *Plasma Med.*, **2018**, 8 (1), 93–120.
- [24] R. Foresti, M. G. Bani-Hani, and R. Motterlini, *Intensive Care Med.*, **2008**, 34 (4), 649–658.
- [25] L. E. Otterbein, F. H. BACH, J. Alam, M. P. SOARES, H. Tao Lu, M. A. WYSK, R. J. DAVIS, R. A. Flavell, A. M. K. K. Choi, H.-T. T. Lu, M. A. WYSK, R. J. DAVIS, R. A. Flavell, A. M. K. K. Choi, R. A. FLAVEL, M. K. AUGUSTINE, CHOI, R. A. Flavell, and A. M. K. K. Choi, *Nat. Med.*, **2000**, 6 (4), 422–428.
- [26] K. Ling, F. Men, W. C. Wang, Y. Q. Zhou, H. W. Zhang, and D. W. Ye, *J. Med. Chem.*, **2018**, 61 (7), 2611–2635.
- [27] R. Motterlini, J. E. Clark, R. Foresti, P. Sarathchandra, B. E. Mann, and C. J. Green, *Circ. Res.*, **2002**, 90 (2), 137–154.

- [28] H. Hokazono and H. Fujimoto, *J. Appl. Phys.*, **1987**, 62 (5), 1585–1594.
- [29] A. Lebouvier, S. A. Iwarere, P. D'Argenlieu, D. Ramjugernath, and L. Fulcheri, *Energy & Fuels*, **2013**, 27 (5), 2712–2722.
- [30] A. Fridman, *Plasma Chemistry*. Cambridge University Press, (2008).
- [31] G. Busco, F. Fasani, S. Dozias, L. Ridou, C. Douat, J.-M. Pouvesle, E. Robert, and C. Grillon, *IEEE Trans. Radiat. Plasma Med. Sci.*, **2018**, 2 (2), 147–152.
- [32] T. C. Manley, *Trans. Electrochem. Soc.*, **1943**, 84 (1), 83.
- [33] A. V. Pipa, J. Koskulics, R. Brandenburg, and T. Hoder, *Rev. Sci. Instrum.*, **2012**, 83 (11), 115112.
- [34] Hui Jiang, Tao Shao, Cheng Zhang, Wenfeng Li, Ping Yan, Xueke Che, and E. Schamiloglu, *IEEE Trans. Dielectr. Electr. Insul.*, **2013**, 20 (4), 1101–1111.
- [35] S. Ponduri, M. M. Becker, S. Welzel, M. C. M. Van De Sanden, D. Loffhagen, and R. Engeln, *J. Appl. Phys.*, **2016**, 119 (9).
- [36] D.-Y. Hwang and A. M. Mebel, *Chem. Phys.*, **2000**, 256 (2), 169–176.
- [37] R. Foresti and R. Motterlini, *Curr. Drug Targets*, **2010**, 11 (12), 1595–1604.
- [38] F. L. Rodkey, T. A. Hill, L. L. Pitts, and R. F. Robertson, *Clin. Chem.*, **1979**, 25 (8), 1388–1393.
- [39] A. Nikam, A. Ollivier, M. Rivard, J. L. Wilson, K. Mebarki, T. Martens, J.-L. Dubois-Randé, R. Motterlini, and R. Foresti, *J. Med. Chem.*, **2016**, 59 (2), 756–762.
- [40] S. Paulussen, B. Verheyde, X. Tu, C. De Bie, T. Martens, D. Petrovic, A. Bogaerts, and B. Sels, *Plasma Sources Sci. Technol.*, **2010**, 19 (3), 034015.
- [41] F. Brehmer, S. Welzel, M. C. M. Van De Sanden, and R. Engeln, *J. Appl. Phys.*, **2014**, 116 (12).
- [42] R. Aerts, T. Martens, and A. Bogaerts, *J. Phys. Chem. C*, **2012**, 116 (44), 23257–23273.
- [43] C. Stewig, S. Schüttler, T. Urbanietz, M. Böke, and A. von Keudell, *J. Phys. D. Appl. Phys.*, **2020**, 53 (12), 125205.
- [44] G. B. Sretenović, O. Guaitella, A. Sobota, I. B. Krstić, V. V. Kovačević, B. M. Obradović, and M. M. Kuraica, *J. Appl. Phys.*, **2017**, 121 (12), 123304.
- [45] G. J. M. M. Hagelaar and L. C. Pitchford, *Plasma Sources Sci. Technol.*, **2005**, 14 (4), 722–733.
- [46] “Phelps database.” [Online]. Disponible : [www.lxcat.net/Phelps](http://www.lxcat.net/Phelps).
- [47] L. Nie, L. Chang, Y. Xian, and X. Lu, *Phys. Plasmas*, **2016**, 23 (9), 093518.
- [48] E. Robert, V. Sarron, D. Riès, S. Dozias, M. Vandamme, and J.-M. Pouvesle, *Plasma*

- Sources Sci. Technol.*, **2012**, 21 (3), 034017.
- [49] S. Wu and X. Lu, *Phys. Plasmas*, **2014**, 21 (12), 123509.
- [50] K. McKay, J.-S. Oh, J. L. Walsh, and J. W. Bradley, *J. Phys. D. Appl. Phys.*, **2013**, 46 (46), 464018.
- [51] U. Kogelschatz, B. Eliasson, and M. Hirth, *Ozone Sci. Eng.*, **1988**, 10 (4), 367–377.
- [52] J.-P. Boeuf, L. L. Yang, and L. C. Pitchford, *J. Phys. D. Appl. Phys.*, **2013**, 46 (1), 015201.
- [53] A. Bogaerts, X. Tu, J. C. Whitehead, G. Centi, L. Lefferts, O. Guaitella, F. Azzolina-Jury, H.-H. Kim, A. B. Murphy, W. F. Schneider, T. Nozaki, J. C. Hicks, A. Rousseau, F. Thevenet, A. Khacef, and M. Carreon, *J. Phys. D. Appl. Phys.*, **2020**, 53 (44), 443001.
- [54] R. Aerts, W. Somers, and A. Bogaerts, *ChemSusChem*, **2015**, 8 (4), 702–716.
- [55] S. Heijkers, R. Snoeckx, T. Kozák, T. Silva, T. Godfroid, N. Britun, R. Snyders, and A. Bogaerts, *J. Phys. Chem. C*, **2015**, 119 (23), 12815–12828.
- [56] T. Kozák and A. Bogaerts, *Plasma Sources Sci. Technol.*, **2014**, 23 (4), 045004.
- [57] A. Ozkan, T. Dufour, T. Silva, N. Britun, R. Snyders, F. Reniers, and A. Bogaerts, *Plasma Sources Sci. Technol.*, **2016**, 25 (5), 055005.
- [58] M. Ramakers, I. Michielsen, R. Aerts, V. Meynen, and A. Bogaerts, *Plasma Process. Polym.*, **2015**, 12 (8), 755–763.
- [59] T. Urbanietz, M. Böke, V. Schulz-Von Der Gathen, and A. Von Keudell, *J. Phys. D. Appl. Phys.*, **2018**, 51 (34).
- [60] J. S. Olson, E. W. Foley, D. H. Mailett, and E. V. Paster, “Measurement of Rate Constants for Reactions of O<sub>2</sub>, CO, and NO with Hemoglobin,” in *Hemoglobin Disorders*, 82, Humana Press, New Jersey, (2003), pp. 065–091.
- [61] H. Jablonowski, A. Schmidt-Bleker, K. Weltmann, T. von Woedtke, and K. Wende, *Phys. Chem. Chem. Phys.*, **2018**, 20 (39), 25387–25398.

## Graphical Abstract

A new method to deliver carbon monoxide (CO) for medical applications is presented. The originality lies in the use of plasma to produce CO locally. In a same device, the beneficial effects of plasma and CO are combined. To assess the delivery of CO from plasma, hemoglobin was used as scavenger of CO and the formation of carboxyhemoglobin (COHb) was quantified. This study reveals for the first time that plasma can generate and deliver CO for therapeutic interventions.

